Heliyon 10 (2024) e31671

Contents lists available at ScienceDirect

Heliyon

journal homepage: www.cell.com/heliyon

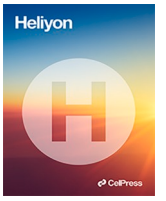

Research article

Antimicrobial topical polymeric films loaded with Acetyl-11-keto-β-boswellic acid (AKBA), boswellic acid and silver nanoparticles: Optimization, characterization, and biological activity

Muhammad Jawad [a], Saurabh Bhatia [a,b,*], Ahmed Al-Harrasi [a,**], Sana Ullah [a], Sobia Ahsan Halim [a,***], Ajmal Khan [a], Esra Koca [c], Levent Yurdaer Aydemir [c], Sevgin Dıblan [d], Anubhav Pratap-Singh [e]

[a] Natural and Medical Sciences Research Center, University of Nizwa, P.O. Box 33, Birkat Al Mauz, Nizwa, 616, Oman
[b] School of Health Science, University of Petroleum and Energy Studies, Dehradun, 248007, India
[c] Department of Food Engineering, Adana Alparslan Turkes Science and Technology University, 01250, Adana, Turkey
[d] Food Processing Department, Vocational School of Technical Sciences at Mersin Tarsus Organized Industrial Zone, Tarsus University, 33100, Tarsus/Mersin, Turkey
[e] BC Food and Beverage Innovation Centre, Faculty of Land & Food Systems, The University of British Columbia, 2205 East Mall, Vancouver, BC-V6T2G2, Canada

ARTICLE INFO

Keywords:
Acetyl-11-keto-β-boswellic acid (AKBA)
Silver nanoparticles (AgNPs)
Carboxymethyl cellulose
Sodium alginate
Gelatin
Antifungal films

ABSTRACT

The study examined the antimicrobial and antioxidant potential of pure Acetyl-11-keto-β-boswellic acid (AKBA), boswellic acid (70%) and AKBA loaded nanoparticles as topical polymeric films. The optimized concentration (0.05 % w/v) of pure AKBA, boswellic acid (BA), and AKBA loaded silver nanoparticles were used to study its impact on film characteristics. Carboxymethyl cellulose (CMC), sodium alginate (SA), and gelatin (Ge) composite films were prepared in this study. The polymeric films were evaluated for their biological (antioxidant and antimicrobial activities) and mechanical characteristics such as tensile strength (TS) and elongation (%). Moreover, other parameters including water barrier properties and color attributes of the film were also evaluated. Furthermore, assessments were conducted using analytical techniques like FTIR, XRD, and SEM. Surface analysis revealed that AgNP precipitation led to a few particles in the film structure. Overall, the results indicate a relatively consistent microstructure. Moreover, due to the addition of AKBA, BA, and AgNPs, a significant decrease in TS, moisture content, water solubility, and water vapor permeation was observed. The films transparency also showed a decreasing trend, and the color analysis revealed decreasing yellowness (b*) of the films. Importantly, a significant increase in antioxidant activity against DPPH free radicals and ABTS cations was observed in the CSG films. Additionally, the AgNP-AKBA loaded films displayed significant antifungal activity against *C. albicans*. Moreover, the molecular docking analysis revealed the inter-molecular interactions between the AKBA, AgNPs, and composite films. The docking results indicate good binding of AKBA and silver nanoparticles with gelatin and

* Corresponding author. Natural and Medical Sciences Research Center, University of Nizwa, P.O. Box 33, Birkat Al Mauz, Nizwa, 616, Oman.
** Corresponding author.
*** Corresponding author.
E-mail addresses: sbsaurabhbhatia@gmail.com (S. Bhatia), aharrasi@unizwa.edu.om (A. Al-Harrasi), sobia_halim@unizwa.edu.om (S.A. Halim).

https://doi.org/10.1016/j.heliyon.2024.e31671
Received 19 January 2024; Received in revised form 20 May 2024; Accepted 20 May 2024
Available online 24 May 2024

carboxymethyl cellulosemolecules. In conclusion, these polymeric films have potential as novel materials with significant antioxidant and antifungal activities.

1. Introduction

Recent trends showed growing interest in phytochemicals due to their safe profile, cost effectiveness and potential biological properties. Acetyl-11-keto-β-boswellic acid (AKBA), is a constituent of the gum exudate derived from *Boswellia sacra*. This phytochemical is known for several biological effects such as antimicrobial, antioxidant, and antiinflmmatory [1–3]. Studies have shown that the AKBA has displayed strong inhibitory action against the leukotriene synthesizing enzyme, 5-lipoxygenase enzyme, which plays a major role in inflammation [4]. Moreover, AKBA is less toxic as compared to other drugs. However, due to its poor water solubility, AKBA has limited biological applications. Additionally, the pre-systemic metabolism greatly reduces the bioavailability of AKBA [5]. To overcome the shortcomings and improve the bioavailability of AKBA, different derivatives such as BA (70 %) and silver nanoparticles (AgNPs) of AKBA were studied to assess the topical delivery of bioactive components using bioadhesive polymeric films.

AgNPs have been reported to have significant biological properties including antiviral, anti-inflammatory, antimicrobial, and wound healing capabilities, therefore, these are considered a significant material with broad potential applications in nanomedicine [6]. AgNPs exhibit various properties including reduced impurities and significantly increased surface-area-to-volume ratios. These unique attributes result in the emergence of novel properties in comparison to silver oxide. Among their notable characteristics, AgNPs demonstrate broad-spectrum bactericidal and fungicidal activities. Additionally, they display proficiency in interacting with various ligands and macromolecules within microbial cells, further enhancing their potential applications in diverse fields [7].

In the current study, composite films using carboxymethyl cellulose (CMC), sodium alginate (SA), and gelatin (Ge) were prepared. Cellulose is an abundantly available biopolymer with an estimated production of around 10^{10}–10^{11} per annum [8]. It is a polydispersed linear polymer composed of poly-β (1,4)-D-glucose units [9], found in hierarchical structures in plant cell walls [10]. Sodium alginate is classified as a linear polysaccharide, derived from alginic acid and isolated from the cell wall of brown seaweed. It is an extremely economical biopolymer composed of α-L guluronic acid (G) and β-D mannuronic acid (M), linked via 1–4 glycosidic bonds [11]. Certain properties of the G-block substantially affect the physicochemical properties of sodium alginate such as molecular weight, length, and composition [12]. Gelatin, a biopolymer sourced from animals like pigs, cows, cattle, and fish, is a non-toxic, water--soluble, and biodegradable protein-based polymer. It originates from collagen, which is the most prevalent protein in mammals [13]. These three polymers exhibit favorable properties for forming gels and films, making them valuable for various applications.

This study focuses on the biological properties of bioadhesive films prepared using pure AKBA, 70 % boswellic acid, and AKBA-loaded silver nanoparticles (AgNPs). The computational study was performed to assess the interaction of different bioactive components with the CMC-SA-Ge film matrix. Moreover, the antioxidant and antimicrobial activities of the films were also evaluated. Additionally, various parameters for the mechanical and barrier properties of the CMC-SA-Ge bioactive films were performed.

2. Materials and Methods

2.1. Materials

Sisco Research Laboratories Pvt Ltd., Mumbai (India) supplied Carboxymethyl cellulose (CMC), sodium alginate (SA) and gelatin (Ge). Glycerol (99 % pure) was supplied by BDH Laboratory Supplies, London (UK).

2.2. Extraction of pure AKBA

The pure oleo-gum resin derived from *Boswellia sacra* was collected from various locations in the Dhofar governorate of Oman and subsequently verified by the herbarium associated with the Natural and Medicinal Sciences Center at the University of Nizwa, Sultanate of Oman. Following authentication, a 400 g sample of air-dried and ground *Boswellia sacra* resin underwent extraction using 100 % methanol (MeOH) for a duration of 2 days, following the procedure outlined by Khan *et al.* [14]. Throughout this extraction process, 285 mg of Acetyl-11-keto-β-boswellic acid (AKBA) was successfully isolated as a UV-active compound, exhibiting a retention time (RT) of 42 min at a flow rate of 4 mL per minute.

2.3. Preparation of ethanolic extract of boswellic acid (BA)

The preparation of 70 % Boswellic acid (BA) was precisely carried out through a series of systematic procedures as outlined by Jauch & Bergmann [15] in their study. Initially, the resin obtained from the *Boswellia sacra* tree underwent hydrodistillation to eliminate the essential oil. Subsequently, the residual matter without essential oil was subjected to ethanol extraction, yielding a boswellic acid-rich oleo gum resin. To further process this enriched oleo gum resin, it was treated with a 0.5 N NaOH solution. The resultant NaOH layer was then acidified using 2 N HCl, which led to the formation of off-white amorphous precipitate. Upon drying this precipitate under vacuum conditions, a powder form of 70 % BA was procured.

2.4. Preparation of AKBA silver nanoparticles

The silver (Ag) nanoparticles (NPs) loaded with AKBA were synthesized utilizing the chemical reduction method described by Khan *et al.* [14]. A solution of 1 mM silver nitrate was made using distilled water, while AKBA was dissolved in methanol. Concurrently, a 3 mM solution of sodium borohydride was prepared in distilled water. The synthesis process involved mixing the noble metal salt with various AKBA ratios and then sequentially adding the 3 mM sodium borohydride solution. This addition was marked by a notable color change in the solution, signaling the formation of silver nanoparticles. To assess stability, the resultant mixtures were set aside for a 24-h period. The presence of nanoparticles was then ascertained using UV–Visible spectrophotometry (BMS (UV-1602), Canada). A 1:1 ratio of silver nitrate to AKBA yielded the most optimal results. The final nanoparticles were centrifuged at 12,000 rpm for a duration of 15 min, then washed using double distilled water to eliminate any residual reducing agent and unbound AKBA.

2.5. Film preparation and composition

The films were prepared using casting techniques. Four samples of the film were made, with one serving as a control (CSG1) and films loaded with Pure AKBA (CSG2), 70 % Boswellic acid (BA) loaded films (CSG3) and AKBA loaded silver nanoparticles (AgNPs) loaded films (CSG4). A 1 % solution of each polymer [Carboxymethyl cellulose (CMC), Sodium Alginate (SA), and Gelatin (Ge)] was formulated by mixing 1 g of the substance in 100 ml of distilled water. The solution of sodium alginate was mixed at room temperature with the aid of a magnetic stirrer. Whereas the solution of gelatin solution was mixed at 55 °C and CMC was mixed at 65 °C. Once the mixtures were prepared, they were uniformly combined. The ratio of CMC, SA, and Ge was 3:1:1 in the film-forming solutions (FFS), respectively. The FFS was separated into four parts (20 ml each) and loaded with different additives. The solutions were labeled as CSG1 (control), CSG2 (Pure AKBA loaded), CSG3 (70 % Boswellic acid), CSG4 (AKBA loaded AgNP), and glycerol (0.8 %) was added as a plasticizer to each sample as per the volume of the solution. Each sample composition is enlisted in Table 1. After proper mixing of the additives in the solution, all the films were cast into petri dishes and left for drying at room temperature (48 h). Chemical structures of the polymers, AKBA, BA and whole scheme for the preparation of films is presented in (Scheme 1).

2.6. Thickness

The thickness of the composite film samples was evaluated using a digital micrometer (Yu-Su 150, Yu-Su Tools). This micrometer offered a high level of accuracy, capable of measuring film samples with a precision of 0.01 mm. To calculate the average thickness, measurements were taken from five locations on each film sample.

2.7. Moisture content

Utilizing the gravimetric method, the moisture content (MC) of CSG films was assessed. Initial weights (W1) were obtained by carefully weighing 3 × 4 cm fragments of the film. These film samples were then subjected to a constant drying temperature of 105 °C until their weights reached uniformity, and the final weights were recorded as (W2). The MC of the CSG films was calculated using the specified formula:

$$MC = \frac{W1 - W2}{W1} \times 100$$

W_1 = initial weight; W_2 = final weight.

2.8. Water vapor permeability (WVP) and water solubility

The gravimetric method, following the procedure outlined by Erdem *et al.* [16] was employed to analyze the water vapor permeability (WVP) of CSG-based films. Glass test cups with dimensions of 5 cm internal diameter and 3 cm depth were utilized in the experiment. Preceding the analysis, the films underwent conditioning in a desiccator set at 50 % relative humidity (RH). To createdifferent RH levels, water (RH = 100 %) and silica gel (RH = 0 %) were utilized. Wrapping tightly around cups filled with silica gel, the control, and pure AKBA, BA (70%), and AKBA AgNPs-loaded edible films were subjected to periodic weight measurements (every 1 h) for a 24-h duration to track weight gain. The water vapor permeability (WVP) was subsequently determined using a specific formula:

Table 1
Detailed chemical composition of pure AKBA, boswellic acid (BA), and AgNPs of AKBA containing bioadhesive films.

Sample code	Composition of Films
CSG1	Carboxymethyl cellulose (1 %)-Sodium Alginate (1 %)-Gelatin (1 %)
CSG2	Carboxymethyl cellulose (1 %)-Sodium Alginate (1 %)-Gelatin (1 %) – Pure AKBA (0.05 % w/v)
CSG3	Carboxymethyl cellulose (1 %)-Sodium Alginate (1 %)-Gelatin (1 %) – BA (70 %) (0.05 % w/v)
CSG4	Carboxymethyl cellulose (1 %)-Sodium Alginate (1 %)-Gelatin (1 %) – AgNPs (0.05 % w/v)

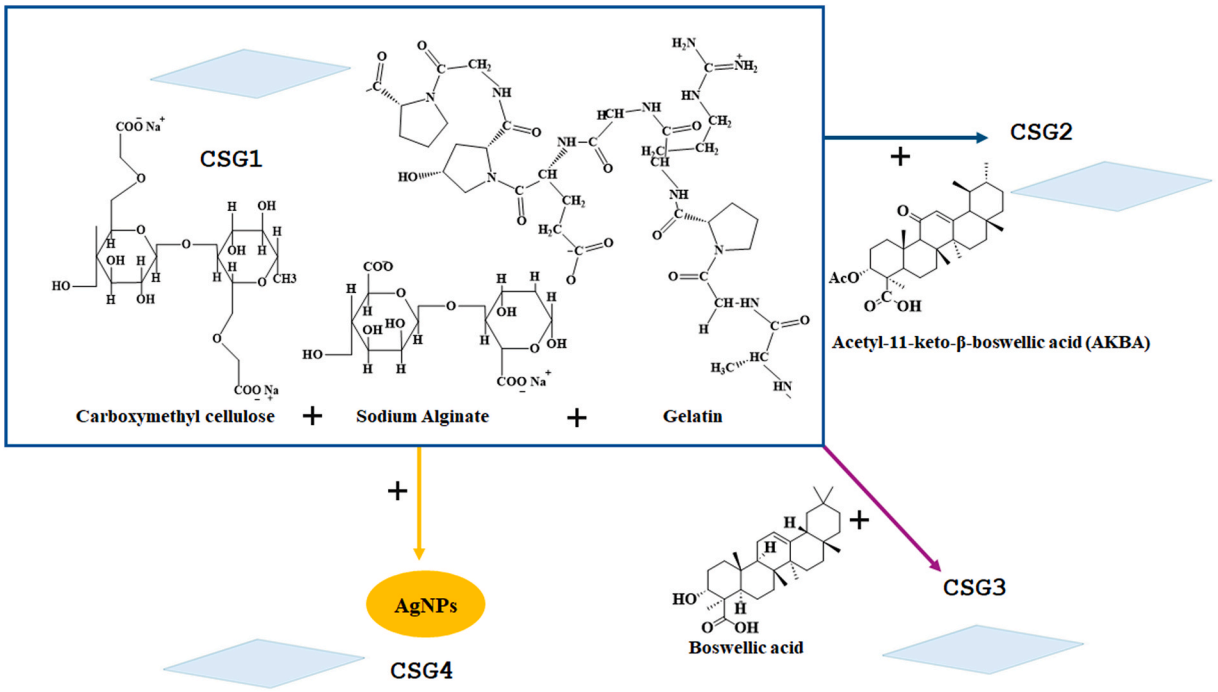

Scheme 1. Presentation of Chemical structures and Composition of Films, developed in this study.

$$WVP = \frac{\Delta m}{\Delta t \times \Delta P \times A} \times d$$

Δm/Δt = weight of moisture gains per unit of time (g/d); A = film area (m^2); ΔP = water vapor pressure difference between the two sides of the film (kPa); d = film thickness (mm).

In order to assess the water solubility (WS) of CSG films, we followed the procedure described by Kim and Song [17]. The strips of edible film measuring 3 × 4 cm was cut and dried in an oven at 105 °C until a constant weight (W1) was achieved and recorded. Following this, the film strips were immersed in 20 ml of distilled water and thoroughly mixed using a shaking incubator (IKA KS3000 IC, IKA®-WerkeGmbH&Co. KG, Staufen, Germany) for a 24-h period. After incubation, the water was drained, and the films underwent another round of drying at 105 °C in an oven. The final weight (W2) was then recorded post-drying, and the calculation of WS utilized the following formula:

$$WS = \frac{W1 - W2}{W1} \times 100$$

W_1 = initial weight; W_2 = final weight.

2.9. Film opacity and color analysis

For the assessment of the opacity of the CSG films, a spectrophotometric technique was employed using Cr-5 Konica Minolta, following the method outlined by Zhao *et al.* [18]. The films were precisely cut into rectangular shapes measuring 4 cm × 1 cm to fit the spectro cuvettes. Subsequently, the transparency of each film was measured at 550 nm using the spectrophotometer. The opacity of the films was then determined using the provided equation:

$$\text{Opacity} = \left(\frac{A550}{x}\right)$$

A_{550} = the absorbance at 550 nm; x = the film thickness (mm).

Following the methodology outlined by Rhim *et al.* [19]., the color analysis of CSG films was performed. The Minolta Colorimeter (CR-300 from Minolta Camera Co., Osaka, Japan), was utilized for the experiment and calibrated using a white calibration plate following the standard procedure. The color properties of the 3 cm edible films were assessed on the Hunter scale (L*, a*, and b*). To ensure precision, the experiments were performed in triplicates. Subsequently, the color difference (ΔE) was calculated based on the obtained values of L*, a*, and b* using the following formula:

$$\Delta E = \sqrt{\Delta L^2 + \Delta a^2 + \Delta b^2}$$

ΔL = L standard − L sample; Δa = a standard − a sample; Δb = b standard − b sample.

2.10. Mechanical properties of the bioadhesive films

Investigation into the mechanical properties of CSG films was carried out in accordance with the ASTM D882 standard methodologies (American Society for Testing and Materials, 2010). The assessment employed a Universal Tester (TA.XT plus, Stable Micro Systems, England) equipped with a 5 kg load cell. Preconditioning of the films occurred within a test cabinet (Nüve TK 120, Türkiye) at 25 °C and 50 % RH for 40 h prior to testing. The edible films were then cut into 7 × 60 mm strips and subjected to mechanical analysis using the instrument, operating at a speed of 6 mm/min. Mechanical properties of the CSG films were evaluated based on two parameters: elongation at break (EAB) (%) and tensile strength (TS) (MPa). To ensure precision, a collection of 5–7 distinct values were recorded, enabling the computation of mean values for both EAB and TS using the respective equations.

$$TS\ (MPa) = \left(\frac{F}{A}\right)$$

F = maximum force; A = cross-sectional area of the film.

$$EAB\ (\%) = \frac{Lf - Li}{Li} \times 100$$

Lf = final length at a break; Li = initial length of the film.

2.11. Scanning electron microscopy

The film images were acquired utilizing a scanning electron microscope (JSM6510LA, Jeol, Japan) set to a voltage of 20 kV. Sample preparation involved placing the films onto aluminum stubs using double-sided adhesive tape. Following this, a fine layer of gold was sputter-coated onto the films, enhancing surface visibility during the imaging procedure.

2.12. Powder X-ray diffraction (PXRD) analysis

The powder X-ray diffraction (PXRD) analysis of films was carried out using the Bruker D8 Discover instrument. The equipment was operated at 40 kV and encompassed a 2-theta (2Θ) angle measurement range spanning from 5 to 50°. Data collection occurred at a scan rate of 0.500 s per data point. The experiment utilized copper (Kα) radiation with a wavelength measuring 1.5418 Å.

2.13. FTIR spectrometry analysis

To assess chemical interactions within the fabricated films, FTIR spectrometry analysis was performed. The FTIR spectra of the films were captured employing an FTIR spectrometer (InfraRed Bruker Tensor 37, Ettlingen, Germany), spanning a wavenumber range of 4000 to 400 cm−1. The experimental procedure entailed data collection at a resolution of 4 cm−1.

2.14. Assays for antioxidant scavenging capacity

In the current investigation, we explored the influence of AKBA and its derivatives on the antioxidant potential of CSG1-CSG4 films using the ABTS and DPPH assays. Adhering to the ABTS assay protocol outlined by Re *et al.* [20], our study followed a standardized procedure. The assessment of ABTS radical scavenging capacity in the tested films (CSG1-CSG4) involved monitoring absorbance changes at 734 nm after 6 min of agitation with 25 mg of film material and 1.9 ml of a 7 mmol/L ABTS radical solution. This solution, containing potassium persulfate at a concentration of 2.45 mM, was prepared according to the described protocol. Results of the antioxidant evaluations were quantified as the percentage inhibition of the ABTS cation radical. The DPPH assay, as per the detailed procedure by Brand-Williams *et al.* [21], involved mixing 75 mg of the test film samples with 1.95 mL of DPPH solution (Sigma-Aldrich, USA). Following vigorous vortexing for 30 s, the mixture underwent a 30-min incubation in a light-protected environment at room temperature. Subsequently, a spectrophotometer measured the solution's absorbance at 517 nm, providing quantitative data on the antioxidant activity of the test samples, expressed as the percentage inhibition of DPPH radicals.

2.15. Antimicrobial assessment

The assessment of the antimicrobial activity of the CSG films was carried out as per the agar diffusion method conducted by Seol *et al.* [22] and Matuschek *et al.* [23]. *Candida albicans* (Fungi) was considered in this study for the assessment of antifungal properties of the CSG films. The fungal strains were activated by incubation in Tryptic soy agar (TSA) for 18 h at 35 °C. The sterile saline solution (0.85 % w/v NaCl) was used to prepare the suspensions of activated *C. albicans* to achieve a 0.5 McFarland turbidity level. Using a cotton swab, the suspension was spread onto Mueller-Hinton agar plates. This resulted in a density of approximately 10^8 colony-forming units (CFU) per milliliter. Circular film samples (diameter 10 mm) were cut and placed onto the Mueller-Hinton agar plates.

Some samples without any antimicrobial agents were included as negative controls. The incubation of plates was carried out for 24–48 h at 35 °C. Subsequently, the clear zones of inhibition surrounding the film discs were quantified in millimeters, encompassing multiple points across the discs. A mean value of the results was considered which signifies the antimicrobial activity of the film samples against the fungal growth.

2.16. Molecular docking studies

Docking was performed by Molecular Operating Environment (MOE version 2022.09). The chemical structures of AKBA (PubChem CID: 11168203) was taken from the PubChem database. While the structures of sodium alginate (β-D-mannuronic acids (M) and α-L-glucuronic (G), linearly linked by 1–4 glycosidic bond) [24], CMC and gelatin [25] were drawn on MOE according to the previous reports. All these molecules were imported into the MOE database of compounds and converted into three-dimensional form through an energy minimization process. We applied MOE's default parameters (RMS gradient of 0.5 kcal/mol/Å, and AM1-BCC charges) for energy minimization. For docking analysis, MOE's default docking method (triangle matcher placement method and London dG scoring method) was used with 100 docked poses of each molecule. Gelatin was selected as the receptor because of its large size, on which each molecule (sodium alginate, CMC, AKBA, and silver nanoparticle) was docked separately and the complex was generated. Based on the highly negative docking score, the most appropriate docked mode (conformation) of each molecule was chosen to visualize their binding interaction on the MOE interface.

2.17. Statistical analysis

To conduct statistical analysis, the mean values, accompanied by their corresponding standard errors, were extracted from three independent replicates. A one-way analysis of variance (ANOVA) was executed to ascertain the significance of variations among the mean values. Following the ANOVA, Duncan's test was applied for post hoc analysis, aimed at pinpointing specific pairwise distinctions. This post hoc test was conducted with a significant level established at 5 %, and a confidence level of 95 %.

3. Results and discussion

3.1. Moisture content

The moisture analysis was carried out for the composite films formulated using CMC, sodium alginate, and gelatin (CSG films). The composite films were loaded with pure AKBA (CSG2), boswellic acid (CSG3), and silver nanoparticles (AgNPs) of AKBA (CSG4). The results revealed that the control CSG film (CSG1) displayed the highest value for MC (30.9). The bioactive films displayed a decrease in MC (CSG2>CSG3>CSG4). The MC of CSG2, CSG3, and CSG4 was observed at 27.8 %, 23.5% and 21.8%. The results are listed in Table 2 AKBA and its derived products might be hydrophobic or less hydrophilic compared to the CSG matrix. This means that these compounds might repel water or have a lower affinity for water, leading to decreased moisture content in the films.

3.2. Thickness

The results of thickness of the films presented in Table 2 reveal a significant decrease in the thickness of CSG films. The control films showed more thickness (0.272 mm) as compared to the loaded films. The thickness of CSG2, CSG3, and CSG4 significantly decreased to 0.2375 mm, 0.202 mm, and 0.184 mm, respectively.

3.3. Water vapor permeability (WVP) and water solubility (WS)

The results of WVP and WS of the CSG composite films are presented in Table 2. The findings indicate that the control CSG films displayed significantly higher (1.22) WVP as compared to the loaded/bioactive films. According to the results, bioactive CSG films had a significantly lower WVP. As observed in Table 2, WVP of CSG2, CSG3, and CSG4 was 1.02, 0.71, and 0.40 ((g*mm)/(m2*h*kPa)), respectively. The results of WS also show a decreasing trend in solubility as various additives are added to the composite films. It can be observed in Table 2 that the solubility decreased from 90.5 % in the control sample (CSG1) to 88.4, 87.4, and 86.6 % in CSG2, CSG3, and CSG4, respectively. This phenomenon can be due to the introduction of hydrophobic AKBA, 70 % BA, and AgNPs, upon which WS and WVP exhibit a marginal decrease. This observed phenomenon could be ascribed to the inherent aromatic configuration of AKBA,

Table 2
Thickness, water solubility (WS), water vapor permeability (WVP), moisture content (MC), and thickness of CSG films.

Sample code	Moisture Content	Water solubility (%)	Thickness (mm)	WVP ((g × mm)/(m2 × h × kPa))
CSG1	30.950 ± 1.58^{a}	90.59 ± 0.10^{a}	0.272 ± 0.040^{a}	1.22 ± 0.17^{a}
CSG2	27.883 ± 1.004^{b}	88.49 ± 1.40^{b}	0.2375 ± 0.026^{a}	1.02 ± 0.02^{a}
CSG3	23.504 ± 1.91^{c}	87.47 ± 0.15^{b}	0.202 ± 0.008^{b}	0.71 ± 0.05^{b}
CSG4	21.867 ± 1.47^{c}	86.67 ± 0.11^{c}	0.184 ± 0.021^{c}	0.40 ± 0.01^{c}

* $^{a\text{-}c}$ represents statistically different values.

implying that AKBA possesses suboptimal water solubility and diminished WVP. Similar results were observed in a study where the effect of organic acid was studied in collagen and chitosan hydrogel composites by Thongchai *et al.* [26].

3.4. Mechanical properties of films

The mechanical strength analysis (Tensile strength and Elongation at break) of the control (CSG1) and bioactive compound loaded films (CSG2, CSG3, CSG4) was conducted in this study, The results of TS revealed a substantial decrease in the strength of the loaded films as compared to the control film (Table 3). CSG1 displayed TS of 3.41 MPa, which was more than CSG2, CSG3 and CSG4. The TS of pure AKBA loaded films (CSG2) was 3.28 MPa, whereas the value decreased to 3.07 MPa for BA loaded films. The TS of AgNPs loaded films was observed to be around 1.84 MPa.

Furthermore, the results of EAB (%) revealed an increase in the loaded films. The control films revealed 69 % EAB. The EAB of pure AKBA-loaded films (CSG2) was observed to be around 143 %. Moreover, the EAB for BA and AgNPs loaded films was noted at 195 % and 248 %, respectively. The results are presented in Table 3. The results suggest that AKBA and the AKBA-derived additives increased the flexibility of the films. The AgNPs of AKBA showed the highest values for EAB as it increased the film flexibility by almost 3.5 folds. Similar results were reported in a previous study where the addition of organic acids (OAs) resulted in a significant increase in the flexibility of the films. Sözbilen et al. [27] observed a concentration-dependent increase in EAB due to the incorporation of different concentrations of OAs.

3.5. Transparency and color analysis

The results of film transparency are presented in Table 4 which reveals a significant decrease in film transparency due to the addition of bioactive components. The film transparency observed in CSG1 was 79.49 %. Furthermore, the results of CSG2, CSG3, and CSG4 showed a decrease in transparency to 77.33 %, 75.57 %, and 69.15 %, respectively. The decrease in transparency observed due to the addition of AKBA, BA and AgNPs of AKBA in the film samples could be linked to the existence of insoluble particles distributed within the resulting composite film [28].

Moreover, the films containing the additives showed the most pronounced color difference when compared to the control samples. The CSG1 (control films) showed a yellow hue, however, with the incorporation of the bioactive components, the yellowness of the films decreased. The overall color difference (ΔE) also decreased due to the incorporation of AKBA and its derivatives. The color difference for control films (CSG1) was 1.93 which decreased to 1.22 in AgNPs-loaded films (CSG4). This observation aligns with earlier research, where adding tea polyphenols [29] and silver nanoparticles [30] led to noticeable color changes in the films.

3.6. Fourier transform infrared (FTIR) spectroscopy

In the Fourier Transform Infrared (FTIR) spectroscopy graph (Fig. 1), the primary absorption peaks represent different functional group vibrations within the CSG composite film. The peak identified at 1031 cm^{-1} in all the samples may be attributable to glycerol [31,32]. The notable absorption peaks observed at 1600 cm^{-1} and 1409 cm^{-1} are linked to the asymmetric and symmetric stretching vibrations of the COO^- group, respectively. Furthermore, the C–*O*–C stretching vibration identified at 1031 cm^{-1} is related to the sugar (saccharide) structure of SA [33,34]. All films exhibit pronounced peaks in the range of 2800–2950 cm−1, which were likely associated with the symmetric and asymmetric stretching vibrations of the CH2 groups in CMC [35]. Moreover, the peaks observed at 1417 cm-1 and 1324 cm-1 are related to amide-III (C–N stretching) and hydroxyl (OH) bending present in CMC [36,37]. Additionally, the notable absorption peaks positioned at 1635 cm−1 might be attributed to Amide I (C–O and N–H stretching vibrations) found in Ge. Furthermore, the broad absorption band around 3200 cm−1 is credited to the stretching vibrations of N–H and O–H [34]. The FTIR spectra of the composite films show sharp peaks with varying amplitudes. However, the integration of AKBA and its derivatives seems to leave the film matrix structure unchanged. Similar results have been reported where no major effect of the structural integrity of the films was observed in FTIR spectra [38].

3.7. Powder X-ray diffraction (PXRD) analysis

Crystalline properties of the CSG composite films, infused with AKBA, BA, and AKBA-loaded AgNPs, were examined using PXRD analysis. As depicted in Fig. 2, a pronounced peak around 20° on the 2θ scale was evident across all samples. This particular peak suggests that the films possess a semi-crystalline character, as reported by Al-Harrasi et al. [39]. To assess the crystallinity, the Diffract

Table 3
Mechanical assessment: tensile strength (TS) and elongation at break (EAB) of CSG films.

Sample code	TS (Mpa)	EAB (%)
CSG1	3.41 ± 0.18^{a}	69 ± 5.24^{a}
CSG2	3.28 ± 0.01^{a}	143 ± 3.04^{b}
CSG3	3.07 ± 0.15^{b}	195 ± 14.35^{c}
CSG4	1.84 ± 0.10^{c}	248 ± 19.22^{d}

*The alphabets ($^{a–d}$) represent statistically different values.

Table 4
Color analysis (L, a*,b*, ΔE) and transparency (%) of CSG films.

Sample Code	L	a*	b*	ΔE	Transparency (%)
CSG1	97.04 ± 0.01[a]	−0.16 ± 0.04[a]	1.72 ± 0.04[a]	1.93 ± 0.04[a]	79.49 ± 1.35[a]
CSG2	96.41 ± 0.11[b]	−0.11 ± 0.01[a]	1.45 ± 0.01[b]	1.42 ± 0.02[b]	77.33 ± 0.98[ab]
CSG3	96.31 ± 0.12[b]	−0.02 ± 0.03[b]	1.32 ± 0.03[c]	1.31 ± 0.03[c]	75.57 ± 0.82[b]
CSG4	95.91 ± 0.04[c]	0.02 ± 0.01[b]	1.17 ± 0.07[d]	1.22 ± 0.06[c]	69.15 ± 1.99[c]

*The alphabets ([a–d]) represent statistically different values.

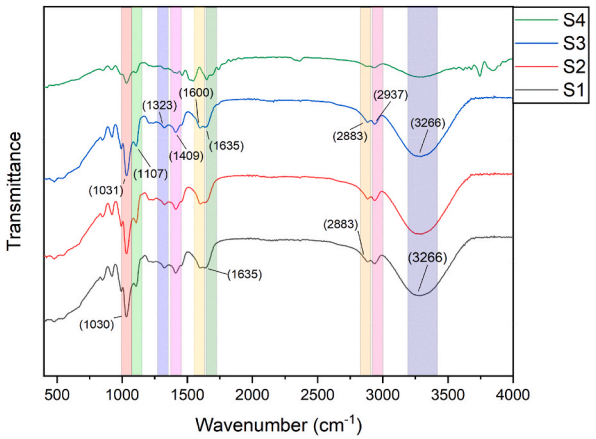

Fig. 1. FTIR analysis of CSG films. CSG1: CMC-SA-Ge control; CSG2: AKBA (0.05 % v/v); CSG3: BA (0.05 % v/v); CSG4: AgNPs (0.05 % v/v).

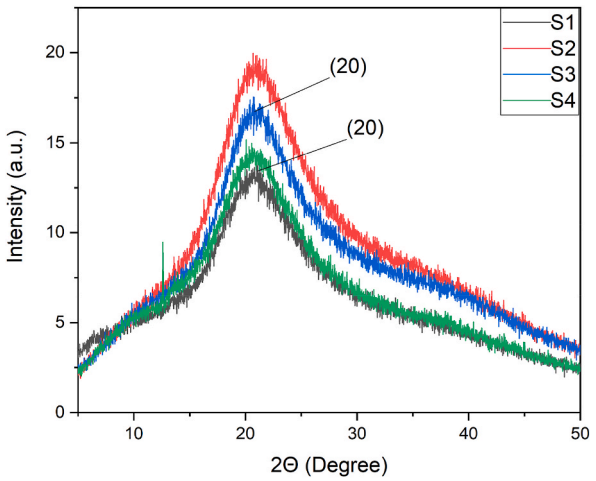

Fig. 2. XRD analysis of CSG films. CSG1: CMC-SA-Ge control; CSG2: AKBA (0.05 % v/v); CSG3: BA (0.05 % v/v); CSG4: AgNPs (0.05 % v/v).

Eva software was employed. The control film sample, S1, displayed a crystallinity of 20.9 %. However, the integration of AKBA (S2), BA (S3), and AgNPs (S4) led to a marginal reduction in the film's crystallinity. The crystallinity levels for S2, S3, and S4 were recorded as 19.2 %, 18.2 %, and 18.9 %, respectively. These findings showed insignificant differences in the crystallinity of the films after the addition of AKBA, BA and AgNPs.

3.8. Scanning electron microscopy (SEM)

The microstructural properties of the film are dependent on the interaction among components of the film that directly impact other properties of the film [50]. To draw the relation between microstructural and other properties of the film SEM (cross-sectional and surface view) was performed as shown in Fig. 3. The surface and cross-sectional images of the films with and without bioactive components revealed no significant difference (Fig. 3). The appearance of the control (CSG1) CMS, SA, and Ge composite displayed a

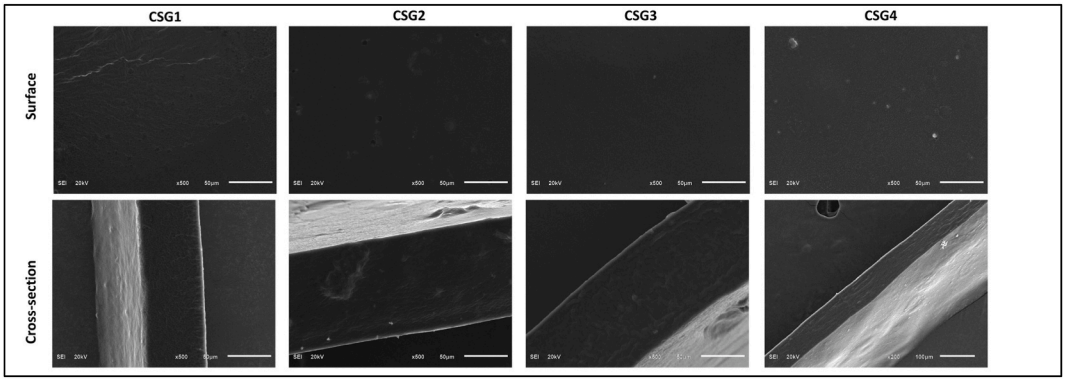

Fig. 3. SEM analysis of CSG films. CSG1: CMC-SA-Ge control; CSG2: AKBA (0.05 % v/v); CSG3: BA (0.05 % v/v); CSG4: AgNPs (0.05 % v/v).

smooth surface with no visible cracks and pores. The SEM analysis also revealed no significant changes in the overall morphology of the films due to the addition of the bioactive components. Only a few immiscible particles were observed in the microstructure of films, but these irregularities did not significantly impact the overall film properties. Surface analysis revealed that AgNP precipitation led to a few particles in the film structure.

3.9. Antioxidant activity of bioactive films

DPPH and ABTS cation scavenging assays were carried out to assess the antioxidant properties of all composite films (Fig. 4). The findings demonstrated that DPPH and ABTS scavenging activities were observed in all films, nevertheless, the activity of the films significantly ($p < 0.05$) increased from CSG1 to CSG4. The incorporation of pure AKBA (CSG2), BA (CSG3), and AgNPs (CSG4) significantly ($p < 0.05$) resulted in higher antioxidant activity than control films (CSG1). CSG1 displayed the lowest antioxidant activity i.e., 16.48 % (DPPH) and 30.8 % (ABTS). The activity significantly increased due to the addition of AKBA and other bioactive components. The antioxidant activity of AKBA and its derivatives has been reported in previous studies. Gupta et al. reported the potent antioxidant activity of *Boswellia serrata* oleo-gum-resin in their recent study [40]. CSG4 showed maximum antioxidant activity against DPPH and ABTS cations since AKBA and AgNPs both have significant antioxidant activity against free radicals [41]. These two powerful antioxidants show significant activity once the nanoparticles are incorporated into the polymeric film matrix of CSG films. CSG4 showed 34.52 % and 54.8 % DPPH and ABTS cation scavenging activity.

3.10. Antimicrobial assay

The antimicrobial activity of CSG films was performed against *Candida albicans* and the findings are presented in Fig. 5. The control CSG films along with films loaded with pure AKBA (CSG2) did not show significant antifungal activity against *C. albicans*. The diameter (mm) of the zone of inhibition (ZOI) BA (CSG3) and AgNPs (CSG4) loaded films were 14.75 ± 0.42 mm and 18.23 ± 1.27 mm, respectively. The ZOI results of the bioactive films against *C. albicans* are presented in Table 5. A maximum ZOI (18.23 mm) was observed in the CSG4 film sample i.e., the AgNPs loaded bioactive films.

AgNPs are reported to have toxic effects due to their oxidative dissolution which generates free silver (Ag) ions. These Ag ions are believed to be the cause of toxicity against microbes [42,43]. The study conducted by Gibala et al. [44] reported similar results for

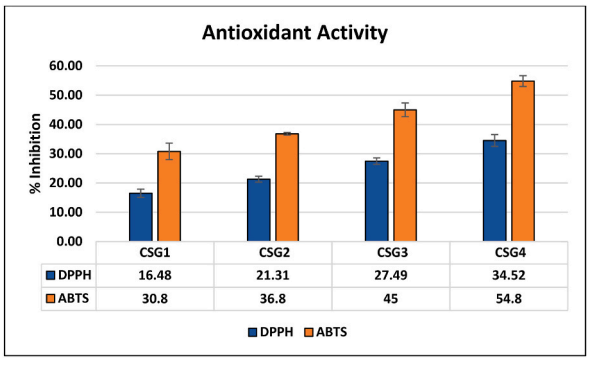

Fig. 4. Antioxidant Assays (DPPH $^{\bullet}$ and ABTS$^{\bullet+}$) to assess the radical scavenging potential of CSG films. CSG1: CMC-SA-Ge control; CSG2: AKBA (0.05 % v/v); CSG3: BA (0.05 % v/v); CSG4: AgNPs (0.05 % v/v).

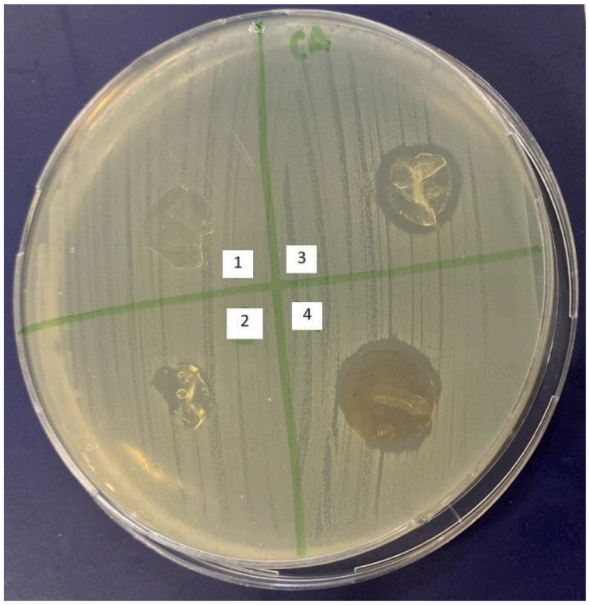

Fig. 5. *Candida albicans* zone of inhibition (included with sample diameter of 10 mm). CSG1: CMC-SA-Ge control; CSG2: AKBA (0.05 % v/v); CSG3: BA (0.05 % v/v); CSG4: AgNPs (0.05 % v/v).

Table 5
Antimicrobial activity against *C. Albicans* of CSG films. CSG1: CMC-SA-Ge control; CSG2: AKBA (0.05 % v/v); CSG3: BA (0.05 % v/v); CSG4: AgNPs (0.05 % v/v).

Sample code	Inhibitory zone (mm)
CSG1	No zone
CSG2	No zone
CSG3	14.75 ± 0.42^{a}
CSG4	18.23 ± 1.27^{b}

Values with different superscript letters in each row are significantly different ($P < 0.05$).

AgNPs against *C. albicans*. Another study carried out by Morones et al. [45] explained the mechanism of action of AgNPs against microorganisms. According to their observation, AgNPs bind to the cell membrane of microbes disturbing their vital functions, including permeation and respiration. The AgNPs also penetrate inside and significantly damage the microbial DNA [45].

3.11. Molecular docking analysis

Docking was employed to investigate the binding interactions of AKBA and Ag-NPs within the composite (cellulose, sodium alginate, and gelatin) film [46]. We observed that the polar moieties of gelatin molecules interact with CMC, SA, and AKBA through hydrogen bonds, while Ag interact with cellulose and gelatin through ionic bonds. The guanidinium and carbonyl groups of gelatin form hydrogen bonds with the –OH of SA (2.29 Å) and the –OH of CMC (2.09 Å), respectively. Moreover, Ag atom is loaded in between gelatin and CMC at <3.0 Å. Within the composite, the amino group of gelatin mediate hydrogen bonds with the carbonyl oxygens of AKBA molecule at 2.37 Å. While the sugar of sodium alginate interact with three –OH groups of CMC at 2.10 to 2.16 Å. The gelatin binds with CMC with docking score of −4.54 kcal/mol, while sodium alginate binds with gelatin-CMC complex with docking score of −5.01 kcal/mol, and the AKBA binds within the composite (gelatin-CMC-sodium alginate complex) with docking score of −4.92 kcal/mol, and this complex accommodates silver atom with docking score of −4.63 kcal/mol. The highly negative docking score indicates excellent and feasible binding of molecules together in the composite. The inter-molecular binding interactions are depicted in Fig. 6.

4. Conclusion

In conclusion, this study emphasizes the promising potential of antifungal topical polymeric films incorporated with pure Acetyl-11-keto-β-boswellic acid (AKBA), Boswellic acid (BA) and silver nanoparticles (AgNPs) of AKBA. The evaluation of the composite of

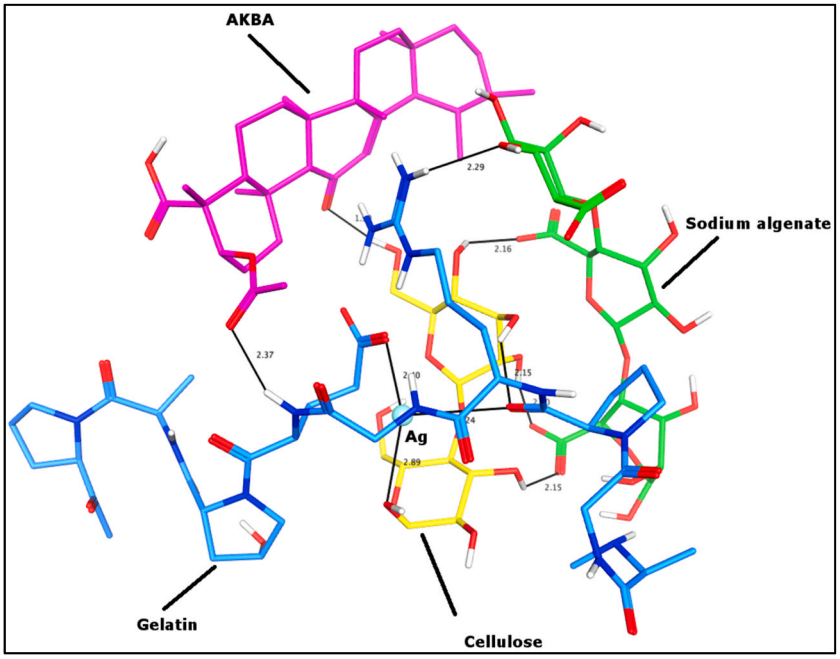

Fig. 6. The inter-molecular interactions between gelatin, carboxymethyl cellulose, sodium alginate, AKBA, and Ag-NP are shown. The molecules are presented in a stick model, while interactions are shown in black lines, and the bond lengths are labeled with the bonds.

Carboxymethyl cellulose (CMC), sodium alginate (SA), and gelatin (Ge) demonstrated consistent microstructure. The films exhibited significant differences in mechanical and physical properties, with a noteworthy decrease in tensile strength and water-related parameters. A significant increase in the biological properties including the antifungal activity and antioxidant capacity of the films was noted, emphasizing the material's potential for biomedical applications. Moreover, the docking study highlighted interactions between AKBA, AgNPs, and the composite film. This research contributes to the understanding of the mechanical, water barrier, and biological properties of composite films with diverse applications.

Funding

The study was supported by TRC grant number BFP/RGP/HSS/22/007.

Institutional review board statement

This study does not contain any studies with human or animal subjects performed by any of the authors.

Data availability statement

Not applicable.

CRediT authorship contribution statement

Muhammad Jawad: Writing – original draft, Methodology, Formal analysis, Data curation. **Saurabh Bhatia:** Writing – review & editing, Supervision, Resources, Project administration, Investigation, Funding acquisition, Conceptualization. **Ahmed Al-Harrasi:** Writing – review & editing, Supervision, Resources, Project administration. **Sana Ullah:** Methodology, Formal analysis, Data curation. **Sobia Ahsan Halim:** Writing – review & editing, Writing – original draft, Visualization, Software, Methodology, Formal analysis, Conceptualization. **Ajmal Khan:** Writing – review & editing, Resources. **Esra Koca:** Writing – original draft, Validation, Methodology, Formal analysis, Data curation. **Levent Yurdaer Aydemir:** Writing – review & editing, Validation, Supervision, Resources, Project administration, Conceptualization. **Sevgin Dıblan:** Writing – original draft, Resources, Methodology, Formal analysis, Data curation, Conceptualization. **Anubhav Pratap-Singh:** Writing – review & editing, Investigation.

Declaration of competing interest

The authors declare that they have no known competing financial interests or personal relationships that could have appeared to

influence the work reported in this paper.

Acknowledgements

The authors are thankful to the Natural and Medical Sciences Research Center, University of Nizwa Oman for providing research facilities to conduct the current study.

References

[1] M. Lv, et al., Acetyl-11-Keto-β-Boswellic acid exerts the anti-cancer effects via cell cycle arrest, apoptosis induction and autophagy suppression in non-small cell lung cancer cells, OncoTargets Ther. (2020) 733–744.
[2] F. Badria, E. Mazyed, Formulation of Nanospanlastics as a promising approach for improving the topical delivery of a natural leukotriene inhibitor (3- acetyl-11-keto-β-boswellic acid): statistical optimization, in vitro characterization, and ex vivo permeation study, Drug Des. Dev. Ther. (2020) 3697–3721.
[3] Y.-q. Liu, et al., Acetyl-11-keto-β-boswellic acid suppresses docetaxel-resistant prostate cancer cells in vitro and in vivo by blocking Akt and Stat3 signaling, thus suppressing chemoresistant stem cell-like properties, Acta Pharmacol. Sin. 40 (5) (2019) 689–698.
[4] D.M. Mostafa, et al., Transdermal microemulsions of Boswellia carterii Bird: formulation, characterization and in vivo evaluation of anti-inflammatory activity, Drug Deliv. 22 (6) (2015) 748–756.
[5] M. Mehta, H. Dureja, M. Garg, Development and optimization of boswellic acid-loaded proniosomal gel, Drug Deliv. 23 (8) (2016) 3072–3081.
[6] A. Santhosh, et al., Green synthesis of silver nanoparticles using cow urine: antimicrobial and blood biocompatibility studies, JCIS Open 3 (2021) 100023.
[7] N. Kokila, et al., Thunbergia mysorensis mediated nano silver oxide for enhanced antibacterial, antioxidant, anticancer potential and in vitro hemolysis evaluation, J. Mol. Struct. 1255 (2022) 132455.
[8] N. Lavoine, et al., Microfibrillated cellulose–Its barrier properties and applications in cellulosic materials: a review, Carbohydr. Polym. 90 (2) (2012) 735–764.
[9] B. Deepa, et al., Biodegradable nanocomposite films based on sodium alginate and cellulose nanofibrils, Materials 9 (1) (2016) 50.
[10] Z. Yu, et al., Chitin-and cellulose-based sustainable barrier materials: a review, Emergent Materials 3 (2020) 919–936.
[11] A. Ahmad, et al., A critical review on the synthesis of natural sodium alginate based composite materials: an innovative biological polymer for biomedical delivery applications, Processes 9 (1) (2021) 137.
[12] K.Y. Lee, D.J. Mooney, Alginate: properties and biomedical applications, Prog. Polym. Sci. 37 (1) (2012) 106–126.
[13] J. Baranwal, et al., Biopolymer: a sustainable material for food and medical applications, Polymers 14 (5) (2022) 983.
[14] A. Khan, et al., Loading AKBA on surface of silver nanoparticles to improve their sedative-hypnotic and anti-inflammatory efficacies, Nanomedicine 14 (21) (2019) 2783–2798.
[15] J. Jauch, J. Bergmann, An efficient method for the large-scale preparation of 3-O-acetyl-11-oxo-β-boswellic acid and other Boswellic acids, Eur. J. Org Chem. 2003 (24) (2003) 4752–4756.
[16] B.G. Erdem, S. Dıblan, S. Kaya, Development and structural assessment of whey protein isolate/sunflower seed oil biocomposite film, Food Bioprod. Process. 118 (2019) 270–280.
[17] S. Kim, K.B. Song, Antimicrobial activity of buckwheat starch films containing zinc oxide nanoparticles against Listeria monocytogenes on mushrooms, Int. J. Food Sci. Technol. 53 (6) (2018) 1549–1557.
[18] J. Zhao, Y. Wang, C. Liu, Film transparency and opacity measurements, Food Anal. Methods 15 (10) (2022) 2840–2846.
[19] J. Rhim, et al., Physical characteristics of a composite film of soy protein isolate and propyleneglycol alginate, J. Food Sci. 64 (1) (1999) 149–152.
[20] R. Re, et al., Antioxidant activity applying an improved ABTS radical cation decolorization assay, Free Radic. Biol. Med. 26 (9–10) (1999) 1231–1237.
[21] W. Brand-Williams, M.-E. Cuvelier, C. Berset, Use of a free radical method to evaluate antioxidant activity, LWT–Food Sci. Technol. 28 (1) (1995) 25–30.
[22] K.-H. Seol, et al., Antimicrobial effect of κ-carrageenan-based edible film containing ovotransferrin in fresh chicken breast stored at 5 C, Meat Sci. 83 (3) (2009) 479–483.
[23] E. Matuschek, D.F. Brown, G. Kahlmeter, Development of the EUCAST disk diffusion antimicrobial susceptibility testing method and its implementation in routine microbiology laboratories, Clin. Microbiol. Infection 20 (4) (2014) O255–O266.
[24] O.D. Frent, et al., Sodium alginate—natural microencapsulation material of polymeric microparticles, Int. J. Mol. Sci. 23 (20) (2022) 12108.
[25] S. Kommareddy, D.B. Shenoy, M.M. Amiji, Gelatin nanoparticles and their biofunctionalization. Nanotechnologies for the Life Sciences, Online, 2007.
[26] K. Thongchai, et al., Characterization, release, and antioxidant activity of caffeic acid-loaded collagen and chitosan hydrogel composites, J. Mater. Res. Technol. 9 (3) (2020) 6512–6520.
[27] G.S. Sözbilen, E. Çavdaroğlu, A. Yemenicioğlu, Incorporation of organic acids turns classically brittle zein films into flexible antimicrobial packaging materials, Packag. Technol. Sci. 35 (1) (2022) 81–95.
[28] S. Galus, J. Kadzińska, Whey protein edible films modified with almond and walnut oils, Food Hydrocolloids 52 (2016) 78–86.
[29] Y. Lei, et al., Investigation of the structural and physical properties, antioxidant and antimicrobial activity of pectin-konjac glucomannan composite edible films incorporated with tea polyphenol, Food Hydrocolloids 94 (2019) 128–135.
[30] D. Kadam, et al., Physicochemical and functional properties of chitosan-based nano-composite films incorporated with biogenic silver nanoparticles, Carbohydr. Polym. 211 (2019) 124–132.
[31] M.S. Hoque, S. Benjakul, T. Prodpran, Effects of partial hydrolysis and plasticizer content on the properties of film from cuttlefish (Sepia pharaonis) skin gelatin, Food Hydrocolloids 25 (1) (2011) 82–90.
[32] Y. Chen, et al., Superhydrophobic coatings on gelatin-based films: fabrication, characterization and cytotoxicity studies, RSC Adv. 8 (42) (2018) 23712–23719.
[33] N. Khuathan, T. Pongjanyakul, Modification of quaternary polymethacrylate films using sodium alginate: film characterization and drug permeability, Int. J. Pharm. 460 (1–2) (2014) 63–72.
[34] L. Yang, et al., Ternary composite films with simultaneously enhanced strength and ductility: effects of sodium alginate-gelatin weight ratio and graphene oxide content, Int. J. Biol. Macromol. 156 (2020) 494–503.
[35] R.K. Deshmukh, et al., Guar gum/carboxymethyl cellulose based antioxidant film incorporated with halloysite nanotubes and litchi shell waste extract for active packaging, Int. J. Biol. Macromol. 201 (2022) 1–13.
[36] N. Singh, et al., Physical properties of zein films containing salicylic acid and acetyl salicylic acid, J. Cereal. Sci. 52 (2) (2010) 282–287.
[37] M.S. Samsi, et al., Synthesis, characterization and application of gelatin–carboxymethyl cellulose blend films for preservation of cherry tomatoes and grapes, J. Food Sci. Technol. 56 (2019) 3099–3108.
[38] W.-H. Huang, et al., Physicochemical characterization, biocompatibility, and antibacterial properties of CMC/PVA/Calendula officinalis films for biomedical applications, Polymers 15 (6) (2023) 1454.
[39] A. Al-Harrasi, et al., Effect of drying temperature on physical, chemical, and antioxidant properties of ginger oil loaded gelatin-sodium alginate edible films, Membranes 12 (9) (2022) 862.
[40] M. Gupta, et al., Correlation of boswellic acids with antiproliferative, antioxidant and antimicrobial activities of topographically collected Boswellia serrata oleo-gum-resin, Phytomedicine 2 (3) (2022) 100289.
[41] Y. Muralidhar, et al., Antibacterial, anti-inflammatory and antioxidant effects of acetyl-11-α-keto-β-boswellic acid mediated silver nanoparticles in experimental murine mastitis, IET Nanobiotechnol. 11 (6) (2017) 682–689.
[42] B. Le Ouay, F. Stellacci, Antibacterial activity of silver nanoparticles: a surface science insight, Nano Today 10 (3) (2015) 339–354.
[43] C. Beer, et al., Toxicity of silver nanoparticles—nanoparticle or silver ion? Toxicol. Lett. 208 (3) (2012) 286–292.

[44] A. Gibała, et al., Antibacterial and antifungal properties of silver nanoparticles—effect of a surface-stabilizing agent, Biomolecules 11 (10) (2021) 1481.
[45] J.R. Morones, et al., The bactericidal effect of silver nanoparticles, Nanotechnology 16 (10) (2005) 2346.
[46] B. Mahesh, et al., Insights into the miscibility characteristics of plastic-mimetic polypeptide with hydroxypropylmethylcellulose: investigation of thermal degradability and intermolecular interactions, Colloids Surf. B Biointerfaces 205 (2021) 111877.